Tuning Superinductors by Quantum Coherence Effects for Enhancing Quantum Computing

Bo Fan,[1,*] Abhisek Samanta,[2,†] and Antonio M. García-García[1,‡]

[1]*Shanghai Center for Complex Physics, School of Physics and Astronomy, Shanghai Jiao Tong University, Shanghai 200240, China*

[2]*Physics Department, Technion, Haifa 32000, Israel*

(Received 6 February 2022; revised 22 September 2022; accepted 6 January 2023; published 24 January 2023)

Research on spatially inhomogeneous weakly coupled superconductors has recently received a boost of interest because of the experimental observation of a dramatic enhancement of the kinetic inductance with relatively low losses. Here, we study the kinetic inductance and the quality factor of a strongly disordered, weakly coupled superconducting thin film. We employ a gauge-invariant random-phase approximation capable of describing collective excitations and other fluctuations. In line with the experimental findings, we have found that in the range of frequencies of interest, and for sufficiently low temperatures, an exponential increase of the kinetic inductance with disorder coexists with a still large quality factor of $\sim 10^4$. More interestingly, on the metallic side of the superconductor-insulator transition, we have identified a range of frequencies and temperatures, $T \sim 0.1 T_c$, where quantum coherence effects induce a broad statistical distribution of the quality factor with an average value that increases with disorder. We expect these findings to further stimulate experimental research on the design and optimization of superinductors for a better performance and miniaturization of quantum devices such as qubit circuits and microwave detectors.

DOI: 10.1103/PhysRevLett.130.047001

A microwave resonator that is both low-loss and small [1–3] is an important element in circuits designed for quantum computation or photon detection. For instance, a high-inductance element [4] suppresses charge fluctuations and slows down electromagnetic waves, which increases coherence times and facilitates the circuit miniaturization. Devices such as the fluxonium qubit [5] have a kinetic inductance $L_{k/\square}$ orders of magnitude larger than the geometrical one related to its shape that is further enhanced by increasing disorder. For that reason, there has been an explosion of interest [5–19] in disordered superconductors as high-inductance devices, commonly called superinductors. Promising results [9–16] have been reported for nanowires of NbN_x, tin, granular Al [20–24], and nanowires of Al based materials [6–8,19].

These materials also have drawbacks. The presence of subgap collective excitations [25–27], especially the Goldstone mode [28] related to phase fluctuations, in highly disordered superconductors [29–33] may shorten coherence times in superconducting circuits. Another potential problem is the existence of strong losses [34,35] in amorphous dielectric due to two level systems. Although this source of decoherence can to some extent be controlled, for instance by reducing the device size [34,35], it can reduce the coherence time of the device. However, the current experimental evidence [11,14] is that this effect is not dominant.

Quantum coherence effects play an important role in weakly coupled disordered superconductors. The order parameter becomes highly inhomogeneous [36–44] with a multifractal-like spatial structure close to the insulating transition leading to the enhancement of superconductivity [36]. Level degeneracies [45–48] cause similar effects in granular materials [40,41] and single superconducting grains. These theoretical findings have been largely confirmed experimentally [20,49–56].

The above results call for a detailed theoretical study of quantum coherence effects in the kinetic inductance and quality factor of disordered superconducting thin films.

In this Letter, we address this problem in a two dimensional weakly coupled disordered superconductor close to the insulating transition but still on the metallic side. We compute these observables by the mean-field limit of the attractive Hubbard model in the weak-coupling limit, namely, the self-consistent Bogoliubov de-Gennes (BdG) formalism [57,58]. Corrections to the BdG formalism are obtained by a random phase approximation leading to gauge-invariant results. Diagrammatically, these deviations correspond to vertex corrections to the mean-field bubble diagrams representing the current-current correlation function. Gauge invariance is necessary in order to reproduce subgap collective excitations such as the Goldstone mode [28] that may increase losses dramatically and therefore prevent the use of disordered superconductors as high-inductance devices. We shall see that, in contrast to previous results [59] on the insulating side of the transition, collective excitations do not occur in the region of interest.

Moreover, in agreement with experiments, the kinetic inductance increases with disorder without a drastic reduction of the quality factor.

Kinetic inductance and quality factor of a superinductor device.—The reactance is defined as $X = 2\pi f L_{k/\Box}$, so a high performance superinductor requires a large kinetic inductance $L_{k/\Box}$. According to the Mattis-Bardeen theory [27], the kinetic inductance of a superconductor is $L_{k/\Box} \sim (\hbar R_{\Box}/\pi\Delta)$, where $R_{\Box}$ is the sheet resistance of the material and Δ is the amplitude of the superconducting order parameter. Therefore, $L_{k/\Box}$ is enhanced by increasing the sheet resistance, which effectively is equivalent to an increase of the disorder strength. However, as mentioned earlier, disorder can also lead to a stronger dissipation at microwave frequencies due to collective modes and other fluctuations [30,32,33] that induce subgap structure in the conductivity near the insulating transition. Therefore, it is important that the enhancement of the kinetic inductance by disorder is not accompanied by these dissipative effects.

Dissipation effects are described by the quality factor $Q = (f/\Delta f)$, where f is the circuit operating frequency (measured in hertz). Q describes the frequency resolution Δf, which is closely related to the strength of dissipative effects leading to electromagnetic absorption and therefore to circuit losses. The total quality factor of the circuit has two components, $(1/Q) = (1/Q_i) + (1/Q_{\mathrm{ext}})$ [60], where Q_i is the internal quality factor computed in this Letter due to losses in the superinductor, and Q_{ext} is the external quality factor related to any other losses. Q_{ext} is typically much higher than Q_i in the experimental settings that we are interested in, so $Q \approx Q_i$.

Two superinductor geometries are especially relevant for applications: superconducting microstrip lines for quantum computing and cavity resonators for phonon detection. We shall see that the main findings of this Letter are applicable to both settings, though Q in each case is different by an overall disorder and temperature independent prefactor. From now on, we focus on the microstrip setup; the cavity resonator is discussed in the Supplemental Material [61]. The quality factor of the microstrip is [62–64] $Q = (\alpha/2\beta)$, where α and β are the real and imaginary parts of the propagation constant γ. For dissipative media, [62,64] $\gamma = \sqrt{i\omega\mu(\sigma + i\omega\epsilon)} = \alpha + i\beta$, where ϵ and μ are the permittivity and permeability of the media, and $\sigma = \sigma_1 - i\sigma_2$ where σ_1 and σ_2 are the real and imaginary parts of the conductivity σ. Since $\sigma_2 \gg \sigma_1$, and the device operates at microwave frequencies [62,63], $Q \approx \sigma_2/\sigma_1$. Likewise, the kinetic inductance is $L_{k/\Box} = (1/2\pi f \sigma_2)$.

Theoretical formalism.—In order to compute $L_{k/\Box}$ and Q, we model the resonator as a disordered superconducting thin film with $N = L \times L$ sites described by the BdG equations [57,58,65,66]

$$\begin{pmatrix} \hat{K} & \hat{\Delta} \\ \hat{\Delta}^* & -\hat{K}^* \end{pmatrix} \begin{pmatrix} u_m(i) \\ v_m(i) \end{pmatrix} = E_m \begin{pmatrix} u_m(i) \\ v_m(i) \end{pmatrix}, \qquad (1)$$

where $\hat{K} u_m(i) = -t\sum_{\delta} u_m(i+\delta) + (V_i - \mu_i)u_m(i)$, V_i is a random potential $V_i \in [-V, V]$, and $\mu_i = \mu + |U|n(i)/2$ is the chemical potential that incorporates the site-dependent Hartree shift, U is the net attractive electronic coupling, and δ is restricted to nearest neighbors of site i. The BdG equations are completed by the self-consistent conditions for the site-dependent order parameter amplitude $\Delta(i) = |U|\sum_m u_m(i)v_m^*(i)[1 - 2f(E_m, T)]$ and the density $n(i) = 2\sum_m[|v_m(i)|^2[1 - f(E_m, T)] + |u_m(i)|^2 f(E_m, T)]$, where $f(E_m, T) = (1/e^{E_m/T} + 1)$ is the Fermi-Dirac distribution at temperature T. The average electron density is $\langle n\rangle = \sum_i n(i)/N = 0.875$ with N the total number of sites of the square lattice. This choice, previously used in [29,65–67], leads to [68] suppression of charge-density wave correlations while keeping the order parameter as large as possible. All these quantities are in units of the hopping energy t. Based on the solutions of these equations, we compute current-current correlation functions beyond the mean-field BdG limit within a gauge-invariant random phase approximation that amounts to considering vertex corrections to the bare bubble diagrams representing the susceptibility. Finally, we compute the complex conductivity from which, as mentioned earlier, it is straightforward to find $Q(T, V, U)$ and $L_{k/\Box}(T, V, U)$ (see Supplemental Material [61] for technical details). Our study is focused on the metallic side of the superconductor-insulator transition, where we will also compute the distribution of probability of Q to assess the role of multifractality and to have an estimate of sample to sample fluctuations that are important in experiments. The choice of parameters in our calculation is motivated by the following considerations. A superconductor resonator typically works in the microwave region 1–20 GHz [2,7,10,69–72], which in units of energy corresponds to 4.0×10^{-3}–8.0×10^{-2} meV. Therefore, we set the hopping energy to $t = 10$ meV so that the operating frequencies of the device lie in the range 1–20 GHz. We will focus on two typical frequencies, $f \sim 0.001t = 0.028\Delta_0$ and $0.004t = 0.112\Delta_0$, corresponding to 2.5 GHz and 10 GHz, respectively. The lattice constant is set to $a = 0.35$ nm and the permittivity $\epsilon = 9\epsilon_0$. We note that all the calculations are carried in SI units, which can be compared to experiments directly. In order to have a larger Q, temperatures must be much lower than the critical one, i.e., $T \ll T_c$, but still accessible experimentally, $T \sim 0.01$–$0.15T_c$. We model weakly coupled superconductors by a coupling constant $U = -1$, in units of t, because this is the smallest coupling for which the finite size effects in our calculation are negligible. For these parameters, we obtain for $V = 0$ an order parameter $\Delta_0 = 0.0357t = 0.357$ meV and a critical temperature $T_c \sim 0.02t \sim 2.3$ K.

Finite-size effects.—We start our analysis of $L_{k/\Box}$ and Q by showing that finite size effects are not important. In Fig. 1, we depict Q for different system sizes L and for two different temperatures. We do not observe any substantial size dependence for $L \geq 26$. Finite size effects in Q are much stronger for small sizes because quantum fluctuations

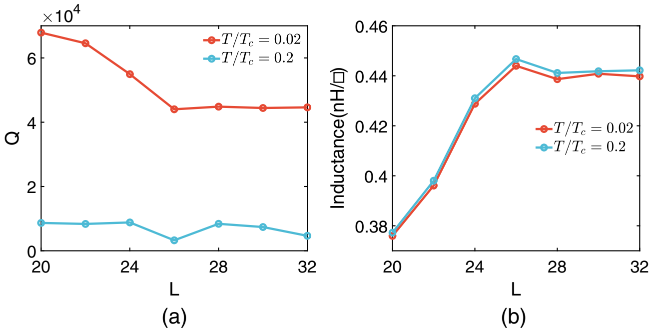

FIG. 1. The quality factor Q (a) and the kinetic inductance $L_{k/\square}$ (b) as a function of system size L for $U = -1$, $\langle n \rangle = 0.875$, $f = 0.028\Delta_0$, and $V = 1.5$, close to the critical disorder, which is the main focus of this Letter. No substantial size dependence is observed for $L \geq 26$, so we fix the size $L = 28$ in our study. For stronger disorder or coupling, finite size effects will be even smaller.

increase as the system size decreases. Finite temperature effects, as observed in Fig. 1, suppress quantum fluctuations. The increase (decrease) of $L_{k/\square}$ (Q) with system size is due to the fact that $L_{k/\square}$ is inversely proportional to σ_2 while Q is directly proportional to it. For a stronger coupling constant $|U| > 1$, finite size effects are smaller because the coherence length is shorter. Therefore, from now on we set $L = 28$.

Temperature, disorder, and frequency dependence of the quality factor.—At sufficiently high temperatures, Q decreases sharply due to the increasing number of thermal quasiparticles [71]. Therefore, this region is not of interest in our analysis. In the superconducting region, $1/Q$ is proportional to the remaining number of thermal quasiparticles, which will be reduced greatly by decreasing temperature [10,71]. As a consequence, Q will increase substantially with decreasing temperature. However, as Fig. 2 shows, this increase levels off for sufficiently low $T \leq 0.1T_c$, which is roughly consistent with experimental results [72]. The origin of this saturation of Q is due to quantum fluctuations [30,32], captured in our analysis by the employed gauge-invariant random phase approximation, that smear out the real conductivity so that it is finite even below the spectral gap. Since Q is a decreasing function of temperature, the optimal operation of the device will always occur at the lowest temperature that can be reached experimentally, though large values of Q can still be observed for $T \sim 0.1T_c$. We note that we are assuming a thermal distribution of quasiparticles but there is substantial evidence that in the low temperature limit, the distribution may be nonthermal [73,74]. However, the quality factor measured experimentally [63] is still quite large $Q > 10^4$, so we do not expect that our main results are altered qualitatively by considering a nonthermal distribution.

Regarding the dependence on disorder, for sufficiently low temperatures, Q decreases sharply as disorder is increased; see Fig. 2. This is expected as both quantum fluctuations and spatial inhomogeneities facilitate the absorption of the incoming electromagnetic radiation and therefore the decrease of Q. Despite this decrease, Q is still large, $\sim 10^4$ for $f \sim 2.5$ GHz and $\sim 5 \times 10^3$ for $f \sim 10$ GHz, in the subgap frequency region of interest provided that the disorder strength is not too strong, $V \lesssim 2$ where V is expressed in units of t. The $V > 2$ insulating region is of no interest for applications. The disorder dependence of Q, for small but finite $T \gtrsim 0.1T_c$, shows an unexpected nonmonotonous behavior in the critical region $V \sim 1.9$; see Fig. 2. In order to fully confirm it, in Fig. 3, we depict Q in linear scale as a function of V. The nonmonotonicity is clearly observed in a relatively small window of temperatures, and only in the critical region $V \simeq 1.9$, but its effect is rather strong. Below, we provide a tentative explanation of this property, which is one of the main results of this Letter. The dependence of Q on frequency is monotonous; it decreases rapidly with increasing frequency. The optimal setting is therefore the smallest frequency that can be accessible to experiments [61].

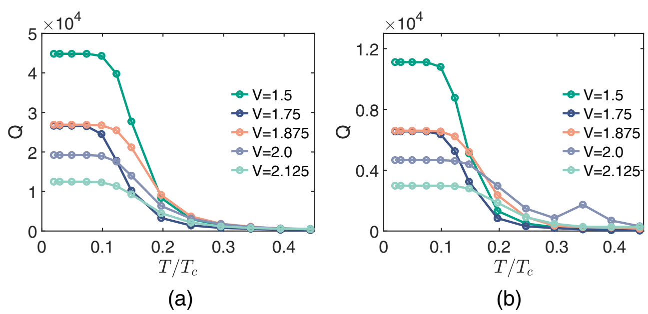

FIG. 2. Quality factor Q as a function of temperature for a lattice of size $L = 28$ and different disorder strengths V, $U = -1$, and $\langle n \rangle = 0.875$. Q is computed using 70 disorder realizations for each V, except for $V = 2.125$, where we employ only 20. The frequency is (a) $f = 0.028\Delta_0 \sim 2.5$ GHz and (b) $f = 0.112\Delta_0 \sim 10$ GHz.

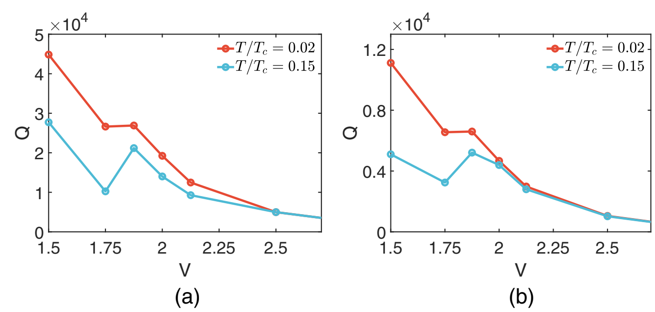

FIG. 3. The quality factor Q as a function of disorder V for $T/T_c = 0.02$ and 0.15 at the experimental frequencies (a) $f \sim 2.5$ GHz and (b) $f \sim 10$ GHz. Q increases with disorder in the critical region close to the transition $V \simeq 1.9$. This nonmonotonicity of Q occurs for others, $T \gtrsim 0.1T_c$ and f, but only for $V \simeq 1.9$. See Fig. 2 for the value of the rest of parameters.

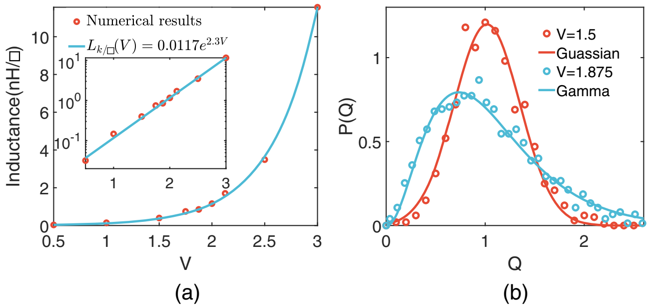

FIG. 4. (a) The kinetic inductance $L_{k/\square}$ as a function of disorder V. The other parameters are the same as those in Fig. 2. The numerical results fit well with an exponential increase of $L_{k/\square}$ with disorder. In the Supplemental Material [61] we show that in the region of interest $f \in [2.5, 10]$ GHz, $T \ll T_c$, $L_{k/\square}$ is almost temperature and frequency independent. (b) Probability distribution of Q from 1000 disorder realizations, normalized by its sample averaged value for $f \sim 2.5$ GHz, and temperature $T/T_c = 0.05$. When $V = 1.5$, the distribution of Q fits well with a Gaussian distribution (red line). However, very close to the transition $V \approx 1.9 \approx V_c$, the distribution, asymmetric and with broad tails, is similar to a Gamma distribution (blue line).

Kinetic inductance.—We now turn to the study of $L_{k/\square}$. The analysis is simpler because it grows monotonically with V and it is weakly dependent on frequency for frequencies below the so called two-particle gap, namely, the frequency required to break a Cooper pair [75]. Since the resistance increases exponentially with disorder, we expect a similar behavior in the kinetic inductance $L_{k/\square}$. In qualitative agreement with the experimental results [6–8,14,76] [see Fig. 4], disorder enhances $L_{k/\square}$ by up to 2 orders of magnitude in the metallic region $V \lesssim 2$ where our formalism is applicable.

Critical disorder and optimal choice of parameters.—Since $L_{k/\square}$ increases sharply with disorder, and a large Q requires $V \leq 2$, it is important to have an estimation of the critical disorder strength V_c at which the insulating transition takes place. The result of an approximate percolation analysis suggests $V_c \sim 2$. This is consistent with an earlier [37] estimate $V_c \sim 1.5$ in a similar system based on level statistics and the vanishing of the superfluid density. At this V, the spectral gap also starts to increase with disorder, which is another indication [65,66] of the transition (see Supplemental Material [61] for more information).

Therefore, based also on the previous results, $V \lesssim 1.9$, corresponding to the strongest disorder still on the metallic side of the transition, is the optimal setting to observe an enhancement of $L_{k/\square}$ without a large decrease in $Q \geq 10^4$. Regarding the rest of the parameters, based on the previous analysis, the optimal conditions for operation of the superinductor are weak-coupling, $|U| \leq 1$, frequencies, $f \sim$ 2.5–10 GHz well below the two-particle spectral gap and the lowest accessible temperature. However, $T \gtrsim 0.15T_c \ll T_c$ is still close to this optimal value and we could also observe in Q an intriguing nonmonotonous dependence on disorder.

With these choices, $L_{k/\square}$ increases up to 2 orders of magnitude with V, and this is not accompanied by strong dissipation since $Q \gtrsim 10^4$ even for $V \lesssim 1.9$. In order to describe quantitatively the experimental results, it would be necessary to have a precise relation between V and the experimental resistivity $\rho_{\rm dc}$ which is a difficult task. We can only say that the region $V \sim 1.9$ of main interest corresponds experimentally to the metallic side of the transition. Perturbatively, $\rho_{\rm dc} \propto \langle V^2 \rangle$ for a noninteracting disordered metal [67].

Discussion and conclusions.—Previously, we found that close to the transition $V_c \simeq 1.9$, and for $T \gtrsim 0.1T_c$, disorder can even enhance the quality factor. We first address the origin of this counterintuitive feature. In principle, by increasing disorder, the order parameter is weakened in parts of the sample that become optically active more easily and lead to the decrease of Q. However, the order parameter spatial distribution close to the transition has multifractal-like features [37,38] like a broad log-normal probability distribution [77], which add a twist to this argument. At zero or low temperature $T \ll T_c$, metallic regions with a large value of the order parameter amplitude coexist with regions where it is close to zero or with incipient Anderson localization effects.

By a slight increase in disorder, it is plausible that regions with a large value of the order parameter remain largely unaltered while the rest may effectively become an Anderson insulator. Unlike metallic but not superconducting regions, those insulating regions do not absorb the incoming electromagnetic radiation. Its net effect is a reduction of optically active regions and therefore an increase of Q with disorder.

As a consequence, the observed sharp drop of Q with temperature occurs at higher temperatures [see Fig. 2(a)], and there exists a relatively narrow region of temperatures, $T \sim 0.15T_c$, for $V \approx V_c$, where the V dependence on Q is nonmonotonic, namely, Q increases with disorder for $V \sim V_c$.

The qualitative changes of Q close to the transition $V_c \simeq 1.9$ (see Fig. 4) are illustrated by computing the probability distribution obtained from 1000 disorder realizations. Even for $V = 1.5$, the distribution is close to a Gaussian. However, for $V_c \approx 1.9$, it becomes broad and asymmetric, signaling large sample to sample fluctuations. This is the region where the order parameter spatial distribution has multifractal-like features, so we believe that the anomalous enhancement of Q is related to this feature. We stress that the employed theoretical formalism is gauge-invariant and therefore can account for collective excitations [26,78] that dramatically lower the quality factor of the device. Indeed, we have found [33] that collective excitations may occur in weakly coupled disordered superconductors. However, it is necessary to have a disorder larger than $V_c \simeq 1.9$ for the collective excitations to be observed for the 2.5–10 GHz frequencies of interest. Therefore, collective excitations do not seem to play any role in the superinductor optimal region of operation.

The coupling we employ, $U = -1$ and $\langle n \rangle = 0.875$, is too strong to describe granular Al [14] experiments. However, we expect similar [79] physics is at play, though the interplay of collective modes and granularity requires a separate study. Note that we neglect Coulomb interactions. It has been recently argued [14,80] that Coulomb interactions may play an important role in granular Al close to the insulating transition. However, on the metallic region of interest, charging effects are screened and therefore do not play an important role.

In conclusion, we have found that strongly disordered, weakly coupled superconducting thin films are excellent superinductors with $L_{k/\square}$ enhanced up to 2 orders of magnitude by disorder while $Q \gtrsim 10^4$. Moreover, close to the superconductor-insulator transition, Q has a broad probability distribution and, counterintuitively, is enhanced by disorder. Despite the limitations mentioned previously, the enhancement of $L_{k/\square}$ with disorder and the mild decrease, and even enhancement in some cases, of Q with disorder is robust, can be confirmed experimentally, and can be used to improve superinductor performance.

B. F. and A. M. G.-G. acknowledge financial support from a Shanghai talent program, from the National Natural Science Foundation China (NSFC) (Grant No. 11874259), and from the National Key R&D Program of China (Project ID: 2019YFA0308603). A. S. acknowledges the computational facilities of Physics Department, Technion.

[*]Corresponding author.
bo.fan@sjtu.edu.cn
[†]Corresponding author.
abhiseks@campus.technion.ac.il
[‡]Corresponding author.
amgg@sjtu.edu.cn

[1] J. Q. You, J. S. Tsai, and Franco Nori, Scalable Quantum Computing with Josephson Charge Qubits, Phys. Rev. Lett. **89**, 197902 (2002).

[2] Xiu Gu, Anton Frisk Kockum, Adam Miranowicz, Yu-xi Liu, and Franco Nori, Microwave photonics with superconducting quantum circuits, Phys. Rep. **718**, 1 (2017).

[3] Morten Kjaergaard, Mollie E. Schwartz, Jochen Braumüller, Philip Krantz, Joel I.-J. Wang, Simon Gustavsson, and William D. Oliver, Superconducting qubits: Current state of play, Annu. Rev. Condens. Matter Phys. **11**, 369 (2020).

[4] J. T. Peltonen, O. V. Astafiev, Yu. P. Korneeva, B. M. Voronov, A. A. Korneev, I. M. Charaev, A. V. Semenov, G. N. Golt'sman, L. B. Ioffe, T. M. Klapwijk, and J. S. Tsai, Coherent flux tunneling through NBN nanowires, Phys. Rev. B **88**, 220506(R) (2013).

[5] Vladimir E. Manucharyan, Jens Koch, Leonid I. Glazman, and Michel H. Devoret, Fluxonium: Single cooper-pair circuit free of charge offsets, Science **326**, 113 (2009).

[6] Anthony J. Annunziata, Daniel F. Santavicca, Luigi Frunzio, Gianluigi Catelani, Michael J. Rooks, Aviad Frydman, and Daniel E. Prober, Tunable superconducting nanoinductors, Nanotechnology **21**, 445202 (2010).

[7] David Niepce, Jonathan Burnett, and Jonas Bylander, High Kinetic Inductance NbN Nanowire Superinductors, Phys. Rev. Appl. **11**, 044014 (2019).

[8] Wenyuan Zhang, K. Kalashnikov, Wen-Sen Lu, P. Kamenov, T. DiNapoli, and M. E. Gershenson, Microresonators Fabricated from High-Kinetic-Inductance Aluminum Films, Phys. Rev. Appl. **11**, 011003(R) (2019).

[9] H. Rotzinger, S. T. Skacel, M. Pfirrmann, J. N. Voss, J. Münzberg, S. Probst, P. Bushev, M. P. Weides, A. V. Ustinov, and J. E. Mooij, Aluminium-oxide wires for superconducting high kinetic inductance circuits, Supercond. Sci. Technol. **30**, 025002 (2017).

[10] Francesco Valenti, Fabio Henriques, Gianluigi Catelani, Nataliya Maleeva, Lukas Grunhaupt, Uwe von Lupke, Sebastian T. Skacel, Patrick Winkel, Alexander Bilmes, Alexey V. Ustinov, Johannes Goupy, Martino Calvo, Alain Benoît, Florence Levy-Bertrand, Alessandro Monfardini, and Ioan M. Pop, Interplay Between Kinetic Inductance, Nonlinearity, and Quasiparticle Dynamics in Granular Aluminum Microwave Kinetic Inductance Detectors, Phys. Rev. Appl. **11**, 054087 (2019).

[11] Lukas Grünhaupt, Nataliya Maleeva, Sebastian T. Skacel, Martino Calvo, Florence Levy-Bertrand, Alexey V. Ustinov, Hannes Rotzinger, Alessandro Monfardini, Gianluigi Catelani, and Ioan M. Pop, Loss Mechanisms and Quasiparticle Dynamics in Superconducting Microwave Resonators Made of Thin-Film Granular Aluminum, Phys. Rev. Lett. **121**, 117001 (2018).

[12] N. Maleeva, L. Grünhaupt, T. Klein, F. Levy-Bertrand, O. Dupre, M. Calvo, F. Valenti, P. Winkel, F. Friedrich, W. Wernsdorfer *et al.*, Circuit quantum electrodynamics of granular aluminum resonators, Nat. Commun. **9**, 1 (2018).

[13] Lukas Grunhaupt, Martin Spiecker, Daria Gusenkova, Nataliya Maleeva, Sebastian T. Skacel, Ivan Takmakov, Francesco Valenti, Patrick Winkel, Hannes Rotzinger, Wolfgang Wernsdorfer *et al.*, Granular aluminium as a superconducting material for high-impedance quantum circuits, Nat. Mater. **18**, 816 (2019).

[14] Aviv Glezer Moshe, Eli Farber, and Guy Deutscher, Granular superconductors for high kinetic inductance and low loss quantum devices, Appl. Phys. Lett. **117**, 062601 (2020).

[15] Patrick Winkel, Kiril Borisov, Lukas Grünhaupt, Dennis Rieger, Martin Spiecker, Francesco Valenti, Alexey V. Ustinov, Wolfgang Wernsdorfer, and Ioan M. Pop, Implementation of a Transmon Qubit Using Superconducting Granular Aluminum, Phys. Rev. X **10**, 031032 (2020).

[16] Fang Yang, Thomas Gozlinski, Tim Storbeck, Lukas Grünhaupt, Ioan M. Pop, and Wulf Wulfhekel, Microscopic charging and in-gap states in superconducting granular aluminum, Phys. Rev. B **102**, 104502 (2020).

[17] O. Dupré, A. Benoît, M. Calvo, A. Catalano, J. Goupy, C. Hoarau, T. Klein, K. Le Calvez, B. Sacépé, A. Monfardini

et al., Tunable sub-gap radiation detection with superconducting resonators, Supercond. Sci. Technol. **30**, 045007 (2017).

[18] S. E. De Graaf, S. T. Skacel, T. Hönigl-Decrinis, R. Shaikhaidarov, H. Rotzinger, S. Linzen, M. Ziegler, U. Hübner, H.-G. Meyer, V. Antonov *et al.*, Charge quantum interference device, Nat. Phys. **14**, 590 (2018).

[19] P. C. J. J. Coumou, E. F. C. Driessen, J. Bueno, C. Chapelier, and T. M. Klapwijk, Electrodynamic response and local tunneling spectroscopy of strongly disordered superconducting tin films, Phys. Rev. B **88**, 180505(R) (2013).

[20] G. Deutscher, H. Fenichel, M. Gershenson, E. Grünbaum, and Z. Ovadyahu, Transition to zero dimensionality in granular aluminum superconducting films, J. Low Temp. Phys. **10**, 231 (1973).

[21] G. Deutscher, M. Gershenson, E. Grünbaum, and Y. Imry, Granular superconducting films, J. Vac. Sci. Technol. **10**, 697 (1973).

[22] B. Abeles, Effect of charging energy on superconductivity in granular metal films, Phys. Rev. B **15**, 2828 (1977).

[23] B. Abeles, Roger W. Cohen, and G. W. Cullen, Enhancement of Superconductivity in Metal Films, Phys. Rev. Lett. **17**, 632 (1966).

[24] Robert Meservey and Paul M. Tedrow, Measurements of the kinetic inductance of superconducting linear structures, J. Appl. Phys. **40**, 2028 (1969).

[25] P. W. Anderson, Random-phase approximation in the theory of superconductivity, Phys. Rev. **112**, 1900 (1958).

[26] P. W. Anderson, Plasmons, gauge invariance, and mass, Phys. Rev. **130**, 439 (1963).

[27] D. C. Mattis and J. Bardeen, Theory of the anomalous skin effect in normal and superconducting metals, Phys. Rev. **111**, 412 (1958).

[28] Jeffrey Goldstone, Field theories with «superconductor» what solutions, Nuovo Cimento (1955–1965) **19**, 154 (1961).

[29] G. Seibold, L. Benfatto, and C. Castellani, Application of the mattis-bardeen theory in strongly disordered superconductors, Phys. Rev. B **96**, 144507 (2017).

[30] T. Cea, D. Bucheli, G. Seibold, L. Benfatto, J. Lorenzana, and C. Castellani, Optical excitation of phase modes in strongly disordered superconductors, Phys. Rev. B **89**, 174506 (2014).

[31] T. Cea, C. Castellani, G. Seibold, and L. Benfatto, Nonrelativistic Dynamics of the Amplitude (Higgs) Mode in Superconductors, Phys. Rev. Lett. **115**, 157002 (2015).

[32] Abhisek Samanta, Amulya Ratnakar, Nandini Trivedi, and Rajdeep Sensarma, Two-particle spectral function for disordered *s*-wave superconductors: Local maps and collective modes, Phys. Rev. B **101**, 024507 (2020).

[33] Bo Fan, Abhisek Samanta, and Antonio M. García-García, Characterization of collective excitations in weakly coupled disordered superconductors, Phys. Rev. B **105**, 094515 (2022).

[34] John M. Martinis, K. B. Cooper, R. McDermott, Matthias Steffen, Markus Ansmann, K. D. Osborn, K. Cicak, Seongshik Oh, D. P. Pappas, R. W. Simmonds, and Clare C. Yu, Decoherence in Josephson Qubits from Dielectric Loss, Phys. Rev. Lett. **95**, 210503 (2005).

[35] Jiansong Gao, The physics of superconducting microwave resonators, Ph.D dissertation, California Institute of Technology, 2008.

[36] James Mayoh and Antonio M. García-García, Global critical temperature in disordered superconductors with weak multifractality, Phys. Rev. B **92**, 174526 (2015).

[37] Bo Fan and Antonio M. García-García, Enhanced phase-coherent multifractal two-dimensional superconductivity, Phys. Rev. B **101**, 104509 (2020).

[38] Bo Fan and Antonio M. García-García, Superconductivity at the three-dimensional anderson metal-insulator transition, Phys. Rev. B **102**, 184507 (2020).

[39] I. S. Burmistrov, I. V. Gornyi, and A. D. Mirlin, Enhancement of the Critical Temperature of Superconductors by Anderson Localization, Phys. Rev. Lett. **108**, 017002 (2012).

[40] James Mayoh and Antonio M. García-García, Number theory, periodic orbits, and superconductivity in nanocubes, Phys. Rev. B **90**, 014509 (2014).

[41] J. Mayoh and A. M. García-García, Strong enhancement of bulk superconductivity by engineered nanogranularity, Phys. Rev. B **90**, 134513 (2014).

[42] I. S. Burmistrov, I. V. Gornyi, and A. D. Mirlin, Superconductor-insulator transitions: Phase diagram and magnetoresistance, Phys. Rev. B **92**, 014506 (2015).

[43] Masaki Tezuka and Antonio M. García-García, Stability of the superfluid state in a disordered one-dimensional ultracold fermionic gas, Phys. Rev A **82**, 043613 (2010).

[44] M. V. Feigel'man, L. B. Ioffe, V. E. Kravtsov, and E. A. Yuzbashyan, Eigenfunction Fractality and Pseudogap State Near the Superconductor-Insulator Transition, Phys. Rev. Lett. **98**, 027001 (2007).

[45] R. H. Parmenter, Size effect in a granular superconductor, Phys. Rev. **166**, 392 (1968).

[46] A. A. Shanenko, M. D. Croitoru, and F. M. Peeters, Oscillations of the superconducting temperature induced by quantum well states in thin metallic films: Numerical solution of the Bogoliubov-de Gennes equations, Phys. Rev. B **75**, 014519 (2007).

[47] Antonio M. García-García, Juan Diego Urbina, Emil A. Yuzbashyan, Klaus Richter, and Boris L. Altshuler, Bardeen-Cooper-Schrieffer Theory of Finite-Size Superconducting Metallic Grains, Phys. Rev. Lett. **100**, 187001 (2008).

[48] Antonio M. García-García, Juan D. Urbina, Emil A. Yuzbashyan, Klaus Richter, and Boris L. Altshuler, BCS superconductivity in metallic nanograins: Finite-size corrections, low-energy excitations, and robustness of shell effects, Phys. Rev. B **83**, 014510 (2011).

[49] C. Brun, T. Cren, V. Cherkez, F. Debontridder, S. Pons, D. Fokin, M. C. Tringides, S. Bozhko, L. B. Ioffe, B. L. Altshuler *et al.*, Remarkable effects of disorder on superconductivity of single atomic layers of lead on silicon, Nat. Phys. **10**, 444 (2014).

[50] Kun Zhao, Haicheng Lin, Xiao Xiao, Wantong Huang, Wei Yao, Mingzhe Yan, Ying Xing, Qinghua Zhang, Zi-Xiang Li, Shintaro Hoshino *et al.*, Disorder induced multifractal superconductivity in monolayer niobium dichalcogenides, Nat. Phys. **15**, 904 (2019).

[51] Carmen Rubio-Verdu, Antonio M. Garcia-Garcia, Hyejin Ryu, Deung-Jang Choi, Javier Zaldivar, Shujie Tang, Bo Fan, Zhi-Xun Shen, Sung-Kwan Mo, Jose Ignacio Pascual, and Miguel M. Ugeda, Visualization of multifractal superconductivity in a two-dimensional transition metal dichalcogenide in the weak-disorder regime, Nano Lett. **20**, 5111 (2020).
[52] Uwe S. Pracht, Nimrod Bachar, Lara Benfatto, Guy Deutscher, Eli Farber, Martin Dressel, and Marc Scheffler, Enhanced cooper pairing versus suppressed phase coherence shaping the superconducting dome in coupled aluminum nanograins, Phys. Rev. B **93**, 100503(R) (2016).
[53] Uwe S. Pracht, Tommaso Cea, Nimrod Bachar, Guy Deutscher, Eli Farber, Martin Dressel, Marc Scheffler, Claudio Castellani, Antonio M. García-García, and Lara Benfatto, Optical signatures of the superconducting goldstone mode in granular aluminum: Experiments and theory, Phys. Rev. B **96**, 094514 (2017).
[54] Sangita Bose, Antonio M. García-García, Miguel M. Ugeda, Juan D. Urbina, Christian H. Michaelis, Ivan Brihuega, and Klaus Kern, Observation of shell effects in superconducting nanoparticles of Sn., Nat. Mater. **9**, 550 (2010).
[55] Zhi Li, Jun-Ping Peng, Hui-Min Zhang, Can-Li Song, Shuai-Hua Ji, Lili Wang, Ke He, Xi Chen, Qi-Kun Xue, and Xu-Cun Ma, Visualizing superconductivity in fese nanoflakes on $srtio_3$ by scanning tunneling microscopy, Phys. Rev. B **91**, 060509(R) (2015).
[56] Ivan Brihuega, Pedro Ribeiro, Antonio M. Garcia-Garcia, Miguel M. Ugeda, Christian H. Michaelis, Sangita Bose, Klaus Kern, and Antonio García-García, Experimental observation of thermal fluctuations in single superconducting Pb nanoparticles through tunneling measurements, Phys. Rev. B **84**, 104525 (2011).
[57] P. G. de Gennes, Boundary effects in superconductors, Rev. Mod. Phys. **36**, 225 (1964).
[58] P. G. de Gennes, *Superconductivity of Metals and Alloys* (W.A. Bebjamin, inc., New York, 1966).
[59] M. V. Feigel'man and L. B. Ioffe, Microwave Properties of Superconductors Close to the Superconductor-Insulator Transition, Phys. Rev. Lett. **120**, 037004 (2018).
[60] Daniel Hafner, Martin Dressel, and Marc Scheffler, Surface-resistance measurements using superconducting stripline resonators, Rev. Sci. Instrum. **85**, 014702 (2014).
[61] See Supplemental Material at http://link.aps.org/supplemental/10.1103/PhysRevLett.130.047001 for discussions about: (i) the theoretical model and the technical details related to the calculation of quality factor and kinetic inductance in disordered superconductors, (ii) temperature dependence of the sample-averaged quality factor and kinetic inductance for different disorder strengths, (iii) the quality factor for a cavity, and (iv) the estimation of critical disorder using the spectral gap and a percolation analysis.
[62] Ghassan Yassin and S Withington, Electromagnetic models for superconducting millimetre-wave and sub-millimetre-wave microstrip transmission lines, J. Phys. D **28**, 1983 (1995).
[63] P. J. de Visser, D. J. Goldie, P. Diener, S. Withington, J. J. A. Baselmans, and T. M. Klapwijk, Evidence of a Nonequilibrium Distribution of Quasiparticles in the Microwave Response of a Superconducting Aluminum Resonator, Phys. Rev. Lett. **112**, 047004 (2014).
[64] D. K. Cheng *et al.*, *Field and Wave Electromagnetics* (Pearson Education India, New York, 1989).
[65] Amit Ghosal, Mohit Randeria, and Nandini Trivedi, Inhomogeneous pairing in highly disordered s-wave superconductors, Phys. Rev. B **65**, 014501 (2001).
[66] Amit Ghosal, Mohit Randeria, and Nandini Trivedi, Role of Spatial Amplitude Fluctuations in Highly Disordered *s*-Wave Superconductors, Phys. Rev. Lett. **81**, 3940 (1998).
[67] Anushree Datta, Anurag Banerjee, Nandini Trivedi, and Amit Ghosal, New paradigm for a disordered superconductor in a magnetic field, arXiv:2101.00220.
[68] Carey Huscroft and Richard T. Scalettar, Evolution of the Density of States Gap in a Disordered Superconductor, Phys. Rev. Lett. **81**, 2775 (1998).
[69] Lukas Grünhaupt, Martin Spiecker, Daria Gusenkova, Nataliya Maleeva, Sebastian T Skacel, Ivan Takmakov, Francesco Valenti, Patrick Winkel, Hannes Rotzinger, Wolfgang Wernsdorfer *et al.*, Granular aluminium as a superconducting material for high-impedance quantum circuits, Nat. Mater. **18**, 816 (2019).
[70] Philip Krantz, Morten Kjaergaard, Fei Yan, Terry P. Orlando, Simon Gustavsson, and William D. Oliver, A quantum engineer's guide to superconducting qubits, Appl. Phys. Rev. **6**, 021318 (2019).
[71] A. V. Sergeev, V. V. Mitin, and B. S. Karasik, Ultrasensitive hot-electron kinetic-inductance detectors operating well below the superconducting transition, Appl. Phys. Lett. **80**, 817 (2002).
[72] Nodar Samkharadze, A. Bruno, Pasquale Scarlino, G. Zheng, D. P. DiVincenzo, L. DiCarlo, and L. M. K. Vandersypen, High-Kinetic-Inductance Superconducting Nanowire Resonators for Circuit QED in a Magnetic Field, Phys. Rev. Appl. **5**, 044004 (2016).
[73] Jhy-Jiun Chang and D. J. Scalapino, Kinetic-equation approach to nonequilibrium superconductivity, Phys. Rev. B **15**, 2651 (1977).
[74] R. E. Horstman and J. Wolter, Gap enhancement in narrow superconducting tunneljunctions induced by homogeneous microwave currents, Phys. Lett. **82A**, 43 (1981).
[75] M. Tinkham, *Introduction to Superconductivity*, 2nd ed. (Dover Publications, Mineola, New York, 2004)
[76] M. Peruzzo, A. Trioni, F. Hassani, M. Zemlicka, and J. M. Fink, Surpassing the Resistance Quantum with a Geometric Superinductor, Phys. Rev. Appl. **14**, 044055 (2020).
[77] James Mayoh and Antonio M. García-García, Global critical temperature in disordered superconductors with weak multifractality, Phys. Rev. B **92**, 174526 (2015).
[78] Yoichiro Nambu, Quasi-particles and gauge invariance in the theory of superconductivity, Phys. Rev. **117**, 648 (1960).
[79] J. R. Waldram, The Josephson effects in weakly coupled superconductors, Rep. Prog. Phys. **39**, 751 (1976).
[80] Aviv Glezer Moshe, Gal Tuvia, Shilo Avraham, Eli Farber, and Guy Deutscher, Tunneling study in granular aluminum near the mott metal-to-insulator transition, Phys. Rev. B **104**, 054508 (2021).